Quantitative estimation of electro-osmosis force on charged particles inside a borosilicate resistive-pulse sensor

Conference Paper · August 2016

DOI: 10.1109/EMBC.2016.7591660

CITATIONS
0

READS
20

5 authors, including:

Mostafa Ghobadi
University at Buffalo, The State University of N…
13 PUBLICATIONS **21** CITATIONS
SEE PROFILE

Ankit Rana
University of Cincinnati
3 PUBLICATIONS **3** CITATIONS
SEE PROFILE

Ehsan Tarkesh Esfahani
University at Buffalo, The State University of N…
51 PUBLICATIONS **175** CITATIONS
SEE PROFILE

Leyla Esfandiari
University of Cincinnati
9 PUBLICATIONS **14** CITATIONS
SEE PROFILE

Quantitative Estimation of Electro-osmosis Force on Charged Particles inside a Borosilicate Resistive-Pulse Sensor

Mostafa Ghobadi* *Student Member, IEEE*, Yuqian Zhang* *Student Member, IEEE*, Ankit Rana, Ehsan T. Esfahani‡, *Member, IEEE,* Leyla Esfandiari‡ *Member, IEEE,*

***Abstract*— Nano and micron-scale pore sensors have been widely used for biomolecular sensing application due to its sensitive, label-free and potentially cost-effective criteria. Electrophoretic and electroosmosis are major forces which play significant roles on the sensor's performance. In this work, we have developed a mathematical model based on experimental and simulation results of negatively charged particles passing through a 2μm diameter solid-state borosilicate pore under a constant applied electric field. The mathematical model has estimated the ratio of electroosmosis force to electrophoretic force on particles to be 77.5%.**

I. Introduction

In the past two decades, nanopore-based sensing, evolved from Coulter counter principle, has gained significant attention in the field of genome sequencing [1-4], molecular sensing [5-8] and medical diagnostics [9,10] due to its intrinsic ultra-sensitive, cost-effective and rapid detection criteria [10]. This sensing scheme is governed by nano-fluidics and electrokinetics in which changes in ionic current were measured from translocation of charged particles driven by an electric field through a small pore [11].

Computational modelling and theoretical analysis of electrokinetics associated with nanopore sensing assist with understanding of fundamental physics and has a significant impact on the sensor's design criteria optimization prior to fabrication. Computational modeling of nanopore-based sensors has been previously demonstrated by other groups [12-16]. For instance, Getpreecharsawas et al. investigated the electric field strength through orifice like pores in an ultrathin membrane [13]. Their theoretical analysis showed that the electric field inside a charged orifice is dependent on the Dukhin number at certain length to diameter aspect ratios. Leburton group fabricated a nanopore in metal-oxide-semiconductor (MOS) capacitor membrane and developed a computational model for simulation of electric response of DNA translocation though the pore [15]. The effect of electroosmosis and the electrophoretic forces on nanoparticles were studied by Dutta group that developed continuum mathematical model to design a separation platform [16]. In another research study, Davenport et al. performed both simulations and experiments to describe the electric field created by the pore's geometry and the applied bias [12]. Kovarik and Jacobson integrated nanopore/microfluidic devices for AC electrokinetic trapping of particles and modeled the electric field distribution across a conical pore using COMSOL multiphysics [14].

Recently, our group, Esfandiari et al demonstrated the binary-mode (yes/no) detection of sequence-specific DNA with the single base mismatch specificity at an impressive concentration detection limit of 10fM utilizing a 2μm diameter borosilicate pore [17, 18]. The device operation was based on the electrophoretic mobility of probe-conjugated beads upon hybridization of negatively charged target nucleic acid (NA) and blockade of the pore by the NA-bead complex which causes a permanent reduction of the current across the pore. In case of the control, non-complementary NA sequence, either no blockade or transient blockade were obtained as a result of the opposing electro-osmosis effect on the reduced charged beads. We have observed that the electrophoretic and electro-osmosis forces play critical roles on the detection accuracy of the sensor by reducing the false negatives (effect of electrophoretic velocity) and the false positives (effect of electro-osmosis). We have previously modeled and calculated the electrophoretic force in our system however, the electro-osmosis of the system is based on the surface charge density of the pore and therefore could not be measured empirically. Here, based on the tracking trajectory of charged microsphere in different positions and the geometry of the pore, a mathematical model is developed to estimate the impede degree caused by electroosmosis flow compared with electrophoretic force on charged particles traveling through a conical pore under the applied electric field.

II. Procedure

A. Materials

Potassium chloride, HEPES, and sodium hydroxide were purchased from Sigma-Aldrich (St. Louis, MO). Silicone elastomer base and silicone elastomer curing agent were obtained from Dow Corning (Elizabethtown, KY). Carboxylic acid-functionalized polystyrene microspheres with diameter of 2.36μm were purchased from Bangs Laboratories, Inc. (Fisher,

* Authors with equal contributions.
‡ Corresponding authors.
Mostafa Ghobadi is with the Department of Mechanical and Aerospace Engineering at University at Buffalo SUNY, Buffalo, NY 14260 USA.
Yuqian Zhang and Ankit Rana are with the department of electrical and computing system, University of Cincinnati, Cincinnati OH.
Ehsan T Esfahani is with the Department of Mechanical and Aerospace Engineering at University at Buffalo SUNY, Buffalo, NY 14260 USA (corresponding author: 716-645-2517; e-mail: ehsanesf@buffalo.edu).
Leyla Esfandiari is with the department of electrical and computing system, University of Cincinnati, Cincinnati OH. USA (corresponding author: 513-556-1355; e-mail: Leyla.esfandiari@uc.edu).

978-1-4577-0220-4/16/$31.00 ©2016 IEEE

IN). Pre-pulled borosilicate glass micropipettes with 2µm were purchased from World Precision Instruments, Inc. (Sarasota, FL)

A. Sensor Apparatus and, Electrical Measurement

2 µm pre-pulled borosilicate pore was back filled with electrolyte solution (1mM KCl and 10mM HEPES, pH 7.0) using a 33 gage Hamilton syringe needle and inserted into a 1mm cylindrical opening that separates two polydimethylsiloxane (PDMS) chambers sealed on a glass slide using Oxygen plasma Cleaning technique (March CS-170). The Pre-pulled borosilicate micropipette with 1mm outer diameter was the only connection between two chambers and to prevent buffer leakage, vacuum grease was used at two connection points of cylindrical opening prior to electrolyte filling of the chambers.

Platinum electrodes were placed into the chambers and 30V DC potential difference was applied using Keithley 2220G-30-1 voltage generator. A trans-impedance amplifier (OPA 111) was used to amplify the output signal. The output current was recorded by acquisition hardware at 1kHz (USB-6361, National Instruments) and LabVIEW software (National Instruments). After recording the baseline current, 10µL of 2.36 µm carboxylate beads diluted in buffer was injected into the borosilicate pore and electrical measurements along with microscopic observation of the bead's mobility was monitored using an inverted fluorescent microscope Nikon Eclipse TE2000-E and captured with high resolution camera Andor NeoZyla 5.5 at a capturing frequency of 100 frames/sec.

The experimental setup was illustrated in Fig. 1-a, where the geometry of the particle when travelling through the pore is depicted in Fig. 1-b.

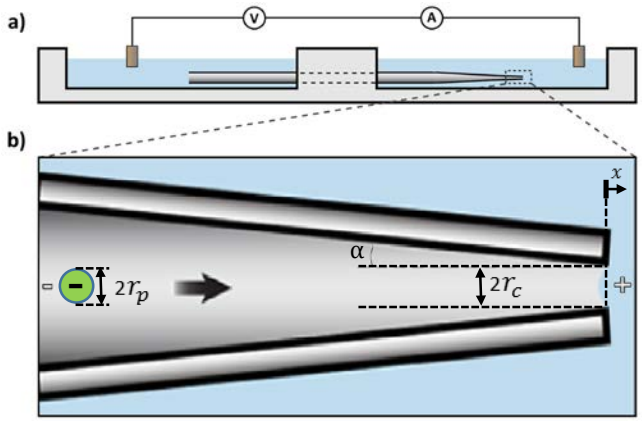

Figure 1. Experimental setup and geometry of particle through micropipette.

B. Tracking the Bead's Motion

The snapshot image of the experiment was used to mark the micropipettes' dimensions on length and width as a calibration reference points to be carried out by the Tracker video analysis and modeling tool built on the Open Source Physics (OSP) Java framework.

Prior to tracking a bead as a point mass, the coordinate axes, as the frame of reference showing with cyan colored perpendicular lines in Fig.2 , were set over the screen at an appropriate edge of the micropipette in the stationary first frame. Following this, a calibration stick was used and placed across the length of the micropipette. The length of the micropipette was measured using the NI toolbox and the same value (in meters) was provided as the length of the stick. Next, a new point mass was created as an object to be tracked and the first frame of the video was marked with the location of the object by a mouse-pointer click. Continuing in the same manner, all the locations of each moving bead were marked frame by frame until it reached the far end of the micropipette and finally went outside crossing the pore. These measurements were repeated five times for each bead's location to capture the uncertainty associated with manual selection. The location of 10 beads passing through the same pore were tracked using this process.

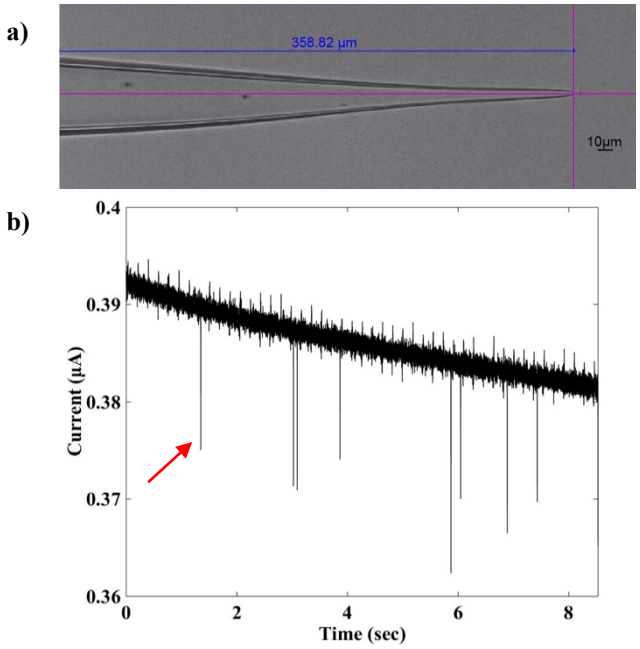

Figure 2. a) The microscopic image of 2 µm diameter micropipette and 2.36 µm beads traveling toward the pore under the electric filed The cyan markers represent tracking position of the beads frame by frame and the blue horizontal marker was the calibration stick. b) Resistive pulses of charged particles pass through the pore, red arrow shows the first pulse.

III. Data Analysis

A method is proposed to estimate the ratio between the electrophoretic force and the portion of drag force affected by electroosmotic flow. The estimation is performed by fitting the motion of the particle predicted by theory to its captured motion from the experiments. Since the motion of the particle through the micropipette is almost one dimensional, the time-position trajectory of particle along *x* direction (See Fig. 1-b) is only considered in this research.

Three main forces are involved in the problem: i) Drag force that resists against the motion of particles, ii) Electrophoretic force which is the only driving force on the particles, and iii) Electroosmotic flow which indirectly affects the motion of particles. In the next section we will study each of these three forces.

A. Drag Force

It is a resisting force against the relative motion of object inside a fluid which is applied as a result of fluid viscosity. According to Stroke's law, the drag force acting on a sphere can be calculated as (1).

$$f_D = 6\pi r_p \eta v_p \quad (1)$$

,where η is the dynamic viscosity of the fluid and r_p and v_p are the radius and velocity vector of the spherical particle, respectively.

B. Electrophoretic force

The electrophoretic force is proportional to the charge of particle (q) as well as the electric field (E) (2).

$$f_{ep}(x) = qE \quad (2)$$

Since the base current remains the same during the motion of particle, the electric potential difference will be $dV = I_b dR$ ($dV = I_b dR$)[17] and the electric field (E), which is by definition the gradient of the electric potential (v), can be written as (3).

$$E(x) = \frac{dV}{dx} = I_b \frac{dR}{dx} \quad (3)$$

, where dR is the resistance of that section of solution material though which the charged particle (q) is passing. This section is always a circular plane with an infinitesimal thickness (dx). We can calculate dR according to the geometry of the capillary (See Fig. 1-b) as shown in (4). It is described in terms of the position of the particle (x) and the following parameters: electrical resistivity (ρ_s), micropipette pore radius (r_c) and slope angle (α).

$$dR = \frac{\rho_s dx}{A(x)} \ , where\ A(x) = \pi(r_c - x\tan(\alpha))^2 \quad (4)$$

Therefore, the electric field can be written as (5).

$$E(x) = \frac{I_b \rho_s}{\pi(r_c - x\tan(\alpha))^2} \quad (5)$$

For a particle being influenced by a constant electric field (E), the interaction of this force and the drag force, will lead to a constant velocity described in (6), where v_{ep} and μ_{ep} are called electrophoretic velocity and mobility, respectively.

$$v_{ep} = \mu_{ep} E$$
$$\mu_{ep} = \frac{q}{6\pi r_p \eta} \quad (6)$$

C. Electroosmotic flow

The zero potential field is an inherent property of the micropipette inner walls which leads to the concentration of cations around the boundary layers of the liquid. This boundary layer is called diffusion layer and therefore has an electric charge. When the charged diffusion layer is exposed to the electric field, it will be driven by the electric force. This causes a sheer force across the diffusion layer with a limited effective distance (less than 200 nm) from the boundary of the fluid that will end up in a steady-state flow of the whole fluid volume with a uniform velocity profile as described by (7).

$$v_{eo}(x) = \mu_{eo} E(x) \quad (7)$$

, where v_{eo} and μ_{eo} present electroosmotic velocity and mobility, respectively. μ_{eo} is calculated by (8), where ϵ_0 and ϵ are vacuum and relative dielectric constants, respectively.

$$\mu_{eo} = \frac{\epsilon_0 \epsilon \zeta}{4\eta} \quad (8)$$

Although this force does not affect the particle directly, its generated fluid motion can indirectly cause a higher or lower drag force. For current problem, electroosmotic force plays a resisting role against the driving electrophoretic force.

D. Equation of motion

The relative velocity of particle inside the fluid is the summation of the bead's inertial velocity and electroosmotic velocity. Therefore, the Newton law for the particle can be written as (9).

$$m\ddot{x} = f_{ep} - f_D = q\,E(x) - 6\pi r_p \eta(\dot{x} + \mu_{eo} E(x)) \quad (9)$$

Using the expression of electric force and electroosmotic fluid described in (5) and (8), the equation of motion can be rewritten as (10).

$$m\ddot{x} + 6\pi r_p \eta\, \dot{x} = \frac{\left(q - \frac{3}{2}\pi\, r_p \epsilon_0 \epsilon \zeta\right) I_b \rho_s}{\pi(r_c - x\tan(\alpha))^2} \quad (10)$$

Since the inertia term is about 10^{-6} smaller than the drag term in practice, the inertia of the particle can be neglected, and therefore, the motion of particle can be simplified to (11).

$$\dot{x} = \frac{k_1}{(x - k_2)^2} \quad (11)$$

All the parameters can be furthered summarized into two parameters k_1 and k_2 described by (12).

$$k_1 = k_{ep} - k_{eo}\ , \qquad k_2 = \frac{r_c}{\tan(\alpha)} \quad (12)$$

, where k_{ep} and k_{eo} represent the coefficient of the electrophoretic and electroosmotic forces and are defined in (13)

$$k_{ep} = \frac{q I_b \rho_s}{6\pi^2 r_p \eta \tan(\alpha)^2}\ , \qquad k_{eo} = \frac{\frac{3}{2}\pi\, r_p \epsilon_0 \epsilon \zeta I_b \rho_s}{6\pi^2 r_p \eta \tan(\alpha)^2} \quad (13)$$

The solution of this simplified equation of motion can be written as either (14) or (15) , where x_0 is the initial position of the particle.

$$t = \frac{(x - k_2)^3 - (x_0 - k_2)^3}{3k_1} \quad (14)$$

$$x = k_2 + \sqrt[3]{3k_1 t + (x_0 - k_2)^3} \quad (15)$$

According to the geometry of the micropipette, k_2 can be calculated in terms of r_c and α. Then, the first parameter (k_1) is estimated by applying nonlinear least square on the error between the measured time-position trajectory of the particle and the expected simulated value.

Using the estimated k_1 and other measured parameters of the experiment (such as q, r_p I_b, ρ_s and η), the ratio (k_v) defined by (16) is introduced that can demonstrate the resisting effect of the electroosmotic flow with respect to the

driving effect of electrophoretic force on the velocity of the particle.

$$k_v = \frac{k_{eo}}{k_{ep}} = \frac{\frac{3}{2}\pi\, r_p \epsilon_0\, \epsilon\, \zeta}{q} = \frac{q - \frac{6\pi^2 r_p \eta \tan(\alpha)^2}{I_b \rho_s} k_1}{q} \qquad (16)$$

IV. Results and Discussion

After estimating the parameters of the motion of particles for all 10 datasets, the trajectories of the particle are reconstructed. Fig. 3 demonstrates that the estimated trajectories do closely fit the measured trajectories. This shows that the motion model of (15), can accurately predict the motion of the particle in real experiments by adjusting only one parameter (k_1). The accuracy of the results not only confirms the theory part, but also provides a reliable estimation of the k_v.

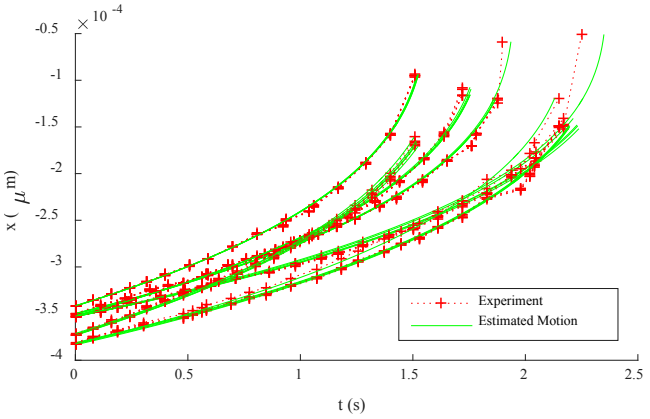

Figure 3. Experimental data versus estimation motions of particle

The histogram of the k_v (ratio of electroosmotic to electrophoretic velocity) is shown in Fig. 4. The mean value of k_v is 77.5%. This value reveals that the order of the magnitude of the drag force produced by electroosmotic flow is significant with respect to the electrophoretic force which should highly be considered in reducing the false positive of the nanopore-based sensor developed by our group [17].

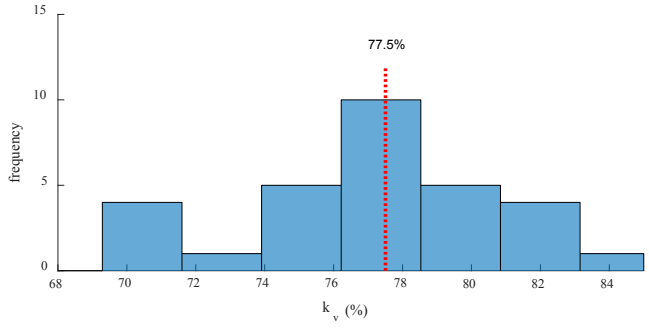

Fig. 4. Histogram of the ratio of resisting velocity generated by electroosmotic flow with respect to the driving electrophoretic force.

Although the nominal size and their surface charge of all the beads used in this study are the same, they are subjected to some level of uncertainty which its effect is seen in the histogram of the k_v.

References

[1] I. M. Derrington, T. Z. Butler, M. D. Collins, E. Manrao, M. Pavlenok, M. Niederweis, and J. H. Gundlach, "Nanopore DNA sequencing with MspA," *Proc. Natl. Acad. Sci.*, vol. 107, no. 37, pp. 16060–16065, Sep. 2010.

[2] C.-S. Ku and D. H. Roukos, "From next-generation sequencing to nanopore sequencing technology: paving the way to personalized genomic medicine," *Expert Rev. Med. Devices*, vol. 10, no. 1, pp. 1–6, Jan. 2013.

[3] D. W. Deamer and M. Akeson, "Nanopores and nucleic acids: prospects for ultrarapid sequencing," *Trends Biotechnol.*, vol. 18, no. 4, pp. 147–151, Apr. 2000.

[4] Y. Astier, O. Braha, and H. Bayley, "Toward single molecule DNA sequencing: Direct identification of ribonucleoside and deoxyribonucleoside 5'-monophosphates by using an engineered protein nanopore equipped with a molecular adapter," *J. Am. Chem. Soc.*, vol. 128, no. 5, pp. 1705–1710, 2006.

[5] S. Howorka and Z. Siwy, "Nanopore analytics: sensing of single molecules," *Chem. Soc. Rev.*, vol. 38, no. 8, p. 2360, 2009.

[6] B. N. Miles, A. P. Ivanov, K. A. Wilson, F. Doğan, D. Japrung, and J. B. Edel, "Single molecule sensing with solid-state nanopores: novel materials, methods, and applications," *Chem. Soc. Rev.*, vol. 42, no. 1, pp. 15–28, 2013.

[7] P. M. Ashton, S. Nair, T. Dallman, S. Rubino, W. Rabsch, S. Mwaigwisya, J. Wain, and J. O'Grady, "MinION nanopore sequencing identifies the position and structure of a bacterial antibiotic resistance island," *Nat. Biotechnol.*, vol. 33, no. 3, pp. 296–300, Dec. 2014.

[8] O. A. Saleh and L. L. Sohn, "An Artificial Nanopore for Molecular Sensing," *Nano Lett.*, vol. 3, no. 1, pp. 37–38, Jan. 2003.

[9] U. M. Mirsaidov, D. Wang, W. Timp, and G. Timp, "Molecular diagnostics for personal medicine using a nanopore," Wiley Interdiscip. Rev. *Nanomedicine Nanobiotechnology*, vol. 2, no. 4, pp. 367–381, Jul. 2010.

[10] B. M. Venkatesan and R. Bashir, "Nanopore sensors for nucleic acid analysis," *Nat. Nanotechnol.*, vol. 6, no. 10, pp. 615–624, Sep. 2011.

[11] Y. Ai and S. Qian, "Electrokinetic particle translocation through a nanopore," *Phys. Chem. Chem. Phys.*, vol. 13, no. 9, p. 4060, 2011.

[12] M. Davenport, K. Healy, M. Pevarnik, N. Teslich, S. Cabrini, A. P. Morrison, Z. S. Siwy, and S. E. Létant, "The Role of Pore Geometry in Single Nanoparticle Detection," *ACS Nano*, vol. 6, no. 9, pp. 8366–8380, Sep. 2012.

[13] J. Getpreecharsawas, J. L. McGrath, and D. A. Borkholder, "The electric field strength in orifice-like nanopores of ultrathin membranes," *Nanotechnology*, vol. 26, no. 4, p. 045704, Jan. 2015.

[14] M. L. Kovarik and S. C. Jacobson, "Integrated Nanopore/Microchannel Devices for ac Electrokinetic Trapping of Particles," *Anal. Chem.*, vol. 80, no. 3, pp. 657–664, Feb. 2008.

[15] M. E. Gracheva, A. Xiong, A. Aksimentiev, K. Schulten, G. Timp, and J.-P. Leburton, "Simulation of the electric response of DNA translocation through a semiconductor nanopore–capacitor," *Nanotechnology*, vol. 17, no. 3, pp. 622–633, Feb. 2006.

[16] T. Z. Jubery, A. S. Prabhu, M. J. Kim, and P. Dutta, "Modeling and simulation of nanoparticle separation through a solid-state nanopore.," *Electrophoresis*, vol. 33, no. 2, pp. 325–33, Jan. 2012.

[17] L. Esfandiari, H. G. Monbouquette, and J. J. Schmidt, "Sequence-specific nucleic acid detection from binary pore conductance measurement.," *J. Am. Chem. Soc.*, vol. 134, no. 38, pp. 15880–6, 2012.

[18] L. Esfandiari, M. Lorenzini, G. Kocharyan, H. G. Monbouquette, and J. J. Schmidt, "Sequence-Specific DNA Detection at 10 fM by Electromechanical Signal Transduction," *Anal. Chem.*, vol. 86, pp. 9638–9643, 2014.